

DR. ADAM MOR (Orcid ID : 0000-0002-2854-2405)

Article type : Original Article

Original Manuscript

Clinical and Experimental Immunology

PLCε1 suppresses tumor growth by regulating murine T cell mobilization

Marianne Strazza ¹, Kieran Adam ¹, Alan Smrcka ², Shalom Lerrer ¹, Adam Mor ^{1,*}

¹ Columbia Center for Translational Immunology, Columbia University Medical Center, New York, NY 10032

² Department of Pharmacology, University of Michigan, Ann Arbor, MI 48109

*** Full Correspondence:**

Adam Mor MD PhD 650 W 168 St. BB-1708, Columbia University Medical Center, New York, NY 10032, USA

am5121@CUMC.Columbia.edu

Disclosure of potential conflicts of interest:

None

This is the author manuscript accepted for publication and has undergone full peer review but has not been through the copyediting, typesetting, pagination and proofreading process, which may lead to differences between this version and the [Version of Record](#). Please cite this article as [doi: 10.1111/cei.13409](https://doi.org/10.1111/cei.13409)

This article is protected by copyright. All rights reserved

Keywords

T cells, chemokines, phospholipase C epsilon 1, murine cancer model, MC38, SDF-1 α .

Abbreviations

PLC ϵ 1: phospholipase C epsilon 1, GEF: guanine nucleotide exchange factor, TCGA: The Cancer Genome Atlas, WT: C57BL/6 wild type, KO: PLC ϵ 1 knockout, LN: lymph nodes, Tcm: central memory T cells, Tem: effector memory T cells, TCR: T cell receptor.

This work was supported by grants from the NIH (AI25640 and CA2312770), and from the Cancer Research Institute.

Abstract

Phospholipase C epsilon 1 (PLC ϵ 1) is a unique member of the phospholipase family in that it also functions as a guanine nucleotide exchange factor (GEF) for the small GTPase Rap1. It is this function as a Rap1 GEF that gives PLC ϵ 1 an essential role in chemokine mediated T cell adhesion. We have utilized a syngeneic tumor model, MC38 cells in C57BL/6 mice, and observed that tumors grow larger and more quickly in the absence of PLC ϵ 1. Single cell analysis revealed an increased CD4⁺/CD8⁺ ratio in the spleens, lymph nodes, and tumors of PLC ϵ 1 knockout tumor-bearing mice. T cells isolated from PLC ϵ 1 knockout mice were less activated by multiple phenotypic parameters than those from wild type mice. We additionally noted a decrease in expression of the chemokine receptors CXCR4 and CCR4 on CD4⁺ T cells from the spleens, lymph nodes, and tumors of PLC ϵ 1 knockout mice compared to wild type mice, and diminished migration of PLC ϵ 1 depleted CD3⁺ T cells toward SDF-1 α . Based on these results we conclude that PLC ϵ 1 is a potential regulator of tumor infiltrating lymphocytes, functioning, at least in part, at the level of T cell trafficking and recruitment.

Introduction

T cell trafficking is a process that is shared by fighting pathogens, autoimmune diseases, and tumor rejection. The directed movement of T cells throughout the body is primarily achieved by specific expression patterns of chemokines and chemokine receptors. In the context of solid tumors, enhancing T cell infiltration is an important therapeutic strategy given our understanding of it being a reliable predictor of patient outcome [1-4]. Research aimed at understanding the tumor microenvironment has gained more traction in recent years, especially as T cell checkpoint inhibitors have proved successful in extending survival of patients unresponsive to other therapies. These therapeutics, including anti-PD-1 and anti-CTLA-4 antibodies, enhance T cell activation in an effort to promote tumor cell identification and elimination [5]. However, without effective T cell recruitment these therapeutics cannot work [6]. The influx of immune cells into the tumor microenvironment can be exploited by the cancer cells and contribute to tumor associated inflammation, thereby promoting tumor growth, progression, and metastasis [7].

Since chemokine and chemokine receptor expression are regulated to maintain specificity of cellular recruitment, these signaling molecules make ideal targets for the selective intervention into T cell infiltration [6, 8, 9]. Many chemokine receptor antagonists that have entered clinical trials have lacked clinical benefit [10-12], likely due to intracellular signaling redundancy among different chemokine pathways, though this redundancy is yet

to be elucidated. Our previous work shows that the enzyme phospholipase C epsilon 1 (PLC ϵ 1) plays a requisite role in CXCR4 signaling in T cells [13]. In a model of contact sensitivity, PLC ϵ 1 knockout mice demonstrated major defect in T cell trafficking and migration. This protein has been implicated in the pathogenesis of numerous diseases [14, 15]. The role of PLC ϵ 1 in tumor progression has primarily been explored in the context of activation state in cancer cells and the contribution to tumor progression from this perspective. The data on PLC ϵ 1 in cancer development and progression has been well reviewed [16]. In this study, we aim to identify the specific contribution of PLC ϵ 1 to T cell tumor infiltration and to the anti-tumor immune response. We report that PLC ϵ 1 plays a necessary role in T cell trafficking and activation in tumor-bearing mice. This work contributes to our understanding of the chemokine signaling network in T cells.

Materials and Methods

Mice and tumor cell lines

Male, 6-8 week-old C57BL/6 (B6) wild type (WT) or PLC ϵ 1 knockout mice (KO) [13, 17] were used in all studies. Animal studies were approved by the New York University institutional animal care and use committee. The WT mice that were used for the control experiments were also used for the KO mice back-crossing, assuring homogeneous genetic background. Mice were housed in the same facility for one week before experiment to synchronize environments. The MC38 colon carcinoma cells were a gift from Ben Neel of New York University. Prior to use, MC38 cells were authenticated by Simple Sequence Length Polymorphism (SSLP). The MC38 cells were maintained in DMEM medium supplemented with heat-inactivated fetal bovine serum (FBS; 10%) and Penicillin-Streptomycin (P/S; 10,000 U/mL stock; 1%) and grown at 37°C with 5% CO₂. Cells were passaged prior to storage and thawed and passaged twice prior to implantation for all described tumor experiments. All cell lines were determined to be free of Mycoplasma (Lonza).

Tumor model

MC38 (1×10^6) cells were implanted subcutaneously in the right hind flank of mice. Tumor growth was monitored using electronic calipers and calculated according to the formula: $V = \text{length} \times \text{width}^2 \times 0.52$. To analyze T cells, spleens, right inguinal lymph nodes, and tumors from both groups were harvested for analysis 14 days post-tumor implantation. For survival experiments, mice were euthanized when tumor size reached $2,000 \text{ mm}^3$ or when tumors became ulcerated. Tumor weight was measured on the day of sacrifice.

Flow cytometry

Cells freshly isolated from murine spleen, right inguinal lymph node, and tumor were stained, non-permeabilized, with fluorescently conjugated antibodies specific for CD3, CD4, CD8, PD-1, CD44, CD62L, CD25, CXCR3, CCR4, CCR7, and CXCR4 (all from Biolegend) in FACS Buffer (PBS without $\text{Ca}^{+2}/\text{Mg}^{+2}$, FBS (2%)). Subsequently, these cells were fixed and permeabilized (True-Nuclear Transcription Factor Buffer Set, Biolegend) to stain with a fluorescently conjugated antibody specific for FoxP3 (Biolegend). Events were recorded using the LSRII (BD) with single stain compensation controls and fluorescence minus one controls. Compensation was done using FACSDiva (BD) and data were analyzed using FlowJo software. Events were first gated based on forward and side scatter, CD3^+ events were then gated and subsequently gated into CD4^+ and CD8^+ populations. CD4^+ and CD8^+ populations were then analyzed for PD-1, CD44, CD62L, CD25, CXCR3, CCR4, CCR7, and CXCR4 expression. Jurkat T cells were stained with APC-conjugated Mouse IgG2a κ or anti-human CXCR4 antibody (Biolegend). Events were recorded using the LSRFortessa (BD) and data were analyzed using FlowJo Software. All flow cytometry analysis was done in adherence with the 'Guidelines for the use of flow cytometry and cell sorting in immunological studies [18].

In vitro CD8⁺ cytotoxicity assay

Splenocytes were isolated from 6-8-week-old B6 wild type or PLC ϵ 1 knockout murine spleens and red blood cells were removed by ACK Lysis Buffer (Lonza). Washed splenocytes were then cultured in complete RPMI medium supplemented with β -mercaptoethanol (55 μM), mouse IL-2 (1,000 IU/mL) and Staphylococcus Aureus

Enterotoxin E (SEE; 1 $\mu\text{g}/\text{mL}$) for 72 hours at a density of 2×10^7 cells/well in a 96 well plate, 37°C with 5% CO_2 . Raji B cells (ATCC) were maintained in complete RPMI media supplemented with heat-inactivated FBS (10%) and P/S (1%) at 37°C with 5% CO_2 . After 72 hours, CD8^+ T cells were isolated from the splenocytes by negative selection (StemCell) and put into co-culture with Raji cells in the presence of IL-2 and SEE at the indicated ratios for 4 hours, after which LDH activity in the supernatant was assayed (Thermo Scientific).

Chemotaxis assay

The chemotaxis of $\text{PLC}\epsilon 1$ depleted T cells toward the chemokine $\text{SDF-1}\alpha/\text{CXCL12}$ (R&D Systems) was assessed using 24-well transwell cell culture inserts with $5\mu\text{m}$ pores (Corning). CD3^+ T cells were isolated through negative selection enrichment kit (Miltenyi). $\text{PLC}\epsilon 1$ depletion was achieved by introducing inhibitory RNA (Dharmacon) as previously described [8]. Control cells were transfected with a scrambled, non-targeting siRNA (Dharmacon). At the start of the assay, T cells were stained with $1\mu\text{M}$ carboxyfluorescein succinimidyl ester (CFSE; Biolegend) and added to the apical compartment of the transwell insert ($100\mu\text{L}$ RPMI media containing 10% fetal bovine serum (FBS), 1.5×10^5 cells/insert). The basolateral compartment was filled with $600\mu\text{L}$ of RPMI containing 10% FBS and $75\text{ ng}/\text{mL}$ $\text{SDF-1}\alpha/\text{CXCL12}$. Chemotaxis was allowed for 3 hours at 37°C with 5% CO_2 . The media and cells from the basolateral compartment were then collected, cells were pelleted, and resuspended in $130\mu\text{L}$ of FACS Buffer to be transferred to a 96 well plate. Cells that moved into the basolateral compartment were quantified by flow cytometry using uniform volume acquisition on the LSRFortessa (BD) and analysis was done using FlowJo Software. Cells were gated based on FSC vs. SSC morphology of primary T cells then based on CFSE positivity. The number of CFSE^+ T cells used to determine the % chemotaxis by dividing the number of CFSE^+ siScramble or si $\text{PLC}\epsilon 1$ CD3^+ T cells by the number of CFSE^+ siScramble cells, therefore normalizing siScramble chemotaxis to 100%.

Statistics

Values are reported as means \pm SEM. Statistical analyses were performed using the Student's t test in GraphPad Prism (ver.7.0c).

Results

PLC ϵ 1 limits MC38 tumor growth and contributes to T cell subset distribution.

Our previous work shows that the enzyme phospholipase C epsilon 1 (PLC ϵ 1) plays a requisite role in CXCR4 signaling in T cells [13]. Within the colorectal cancer samples included in The Cancer Genome Atlas (TCGA) (http://www.oncolnc.org/kaplan/?lower=33&upper=33&cancer=READ&gene_id=51196&raw=plce1&species=mRNA), high PLC ϵ 1 expression correlates with greater five-year survival (Supporting Information Fig. 1a). We implanted MC38 cells into C57BL/6 wild type (WT) or PLC ϵ 1 knockout (KO) mice and observed that tumors grew larger in the KO mice (Fig. 1a and Supporting Information Fig. 1b). We next isolated cells from the tumors, right inguinal lymph nodes (LN), and spleens of mice 14 days after MC38 cell implantation or spleens of non-tumor-bearing mice and analyzed by flow cytometry. In the spleens of non-tumor-bearing mice CD4⁺/CD8⁺ ratios were equivalent between WT and KO mice (Fig. 1b). Following 14 days of tumor growth, the CD4⁺/CD8⁺ ratio in the spleens decreased in WT mice though not in KO mice (Fig. 1c). Likewise, the CD4⁺/CD8⁺ ratio was higher in the LN and tumors of KO mice compared to the same sites in WT mice (Fig. 1d, e). At all sites, the increase in CD4⁺ T cells could not be accounted for by regulatory T cells as there was no difference observed in this subset (Supporting Information Fig. 2).

Activation of tumor infiltrating T cells requires PLC ϵ 1.

To assess the activation state of the CD4⁺ and the CD8⁺ cells, we determined surface expression of CD44, CD62L, and PD-1. Overall, significantly fewer KO CD4⁺ T cells expressed CD44 and PD-1 in the spleens, LN, and tumors (Fig. 2a and Supporting information Fig. 3). Additionally, there was an increased presence of naïve CD4⁺ T cells (Naïve; CD62L⁺ CD44⁻) at all three sites (Fig. 2b). Fewer CD44⁺ CD8⁺ T cells were observed isolated from the spleens, LN, and tumors of KO mice (Fig. 2c). The majority of CD8⁺ T cells isolated from all sites in KO mice were naïve, with a near absence of central memory (T_{cm}; CD62L⁺ CD44⁺) and effector memory (T_{em}; CD62L⁻ CD44⁺) populations (Fig. 2d), demonstrating overall lower activation in the absence of PLC ϵ 1. Unexpectedly, and unlike

the CD4⁺ infiltrating T cells, many of the CD8⁺ infiltrating T cells were negative for PD-1 (Fig. 2d).

Infiltrating T cells express different chemokine receptors in the absence of PLC ϵ 1.

This observation of lower T cell activation could be due to a role for PLC ϵ 1 in T cell receptor (TCR) signaling, or due to improper localization with other cells in the microenvironment. Accordingly, we isolated CD8⁺ T cells and assessed nonspecific cytotoxic activity. Nevertheless, PLC ϵ 1 KO T cells could induce Raji cell cytotoxicity to the same extent as WT CD8⁺ T cells in the presence of super antigen SEE (Fig. 3a). This suggests that PLC ϵ 1 does not contribute to T cell effector function, and leaves open the possibility that cellular mislocalization to or within the tumor is responsible for the observed lack of activation.

When assessing the expression levels of various chemokine receptors on the surface of T cells isolated from the spleens, LN, and tumors we found that fewer KO CD4⁺ T cells isolated from the spleens and tumors expressed CCR4 (Fig. 3b). Within the LN fewer CD4⁺ T cells expressed CCR4 in KO mice, though differences were less pronounced due to overall lower CCR4 positivity in both genotypes. Additionally, fewer CD4⁺ T cells expressed CXCR4 in the spleens, LN, and tumors of KO mice (Fig. 3b), suggesting that CCR4 and CXCR4 are critically contributing to T cell recruitment in this model. No consistent difference in the low level of CXCR3 expression on CD4⁺ T cells was observed. Analysis of CXCR4, CCR4, and CXCR3 expression on CD8⁺ T cells did not uncover any differences (Supporting Information Fig. 4). This finding is consistent with the increased CD4⁺ T cell presence observed in KO mice (Fig. 1). No differences were observed in the expression of CCR7. Mechanistically, we also identified a defect in the PLC ϵ 1 deficient CD4⁺ T cells migrating toward the CXCR4 ligand SDF-1 α (Fig. 3c). Importantly, no change in CXCR4 surface expression was detected when PLC ϵ 1 was knocked down (Supporting Information Fig. 5), suggesting that the defect in migration is due to signaling differences downstream of CXCR4. This data combined with the observation of fewer CCR4⁺ and CXCR4⁺ T cells in the study sites of PLC ϵ 1 KO mice might suggest that these cells are unable to utilize these pathways to traffic to these sites.

Overall, our data indicate a potential role for CCR4 and CXCR4 pathways in T cell localization within the tumor, and a role for PLC ϵ 1 in these signaling cascades.

Discussion

Overall, this study is descriptive and preliminary. While it does not provide definitive proof of mechanism, it should be regarded as hypothesis generating. We hypothesize that further development of this work will demonstrate a role for the enzyme PLC ϵ 1 in T cell distribution throughout multiple anatomical sites in tumor-bearing mice. Our finding that CD4⁺ T cells are more abundant, less activated, and express lower levels of CXCR4 and CCR4 in the spleens, LN, and tumors of PLC ϵ 1 KO mice proposes to us that the overall trafficking of these cells relies on PLC ϵ 1 function. While both CD4⁺ and CD8⁺ T cell frequencies are altered in the absence of PLC ϵ 1 the observed chemokine receptor differences were preferentially within the CD4⁺ subset. Two possible explanations for this distinction are that either the disruption of CD4⁺ T cell migration and activation precedes and precludes CD8⁺ T cell activation and proliferation or that other PLC ϵ 1 dependent chemokine receptors not quantified in this study may be preferentially expressed on CD8⁺ T cells. To address these hypotheses, more extensive and conclusive analysis of these pathways must be done.

We propose that PLC ϵ 1 is active downstream of CCR4, as we have shown previously for CXCR4 [13], and that these pathways may play critical roles in the proper localization of CD4⁺ T cells within the tumor microenvironment. We have shown previously that the impact of PLC ϵ 1 loss on inflammation was T cell intrinsic [13], though the indirect role for PLC ϵ 1 may be more widespread. For example, one ligand for CCR4 is CCL2 which also binds the receptor CCR2, a chemokine receptor that is expressed highly on M2-like macrophages. In fact, CCL2-CCR2 engagement on macrophages has been shown to contribute to anti-inflammatory polarization of macrophages with higher IL-10 production [19], poor antigen presentation, and promotion of new blood vessel growth [20]. Each of these outcomes could lead to enhanced tumor growth. Lower levels of CCR4 on T cells within the same tumor microenvironment could lead to higher local levels of CCL2 available to interact with

CCR2 on macrophages. Accordingly, we cannot rule out that PLC ϵ 1 also plays a role in other types of immune cells.

This work is not free of limitations. Flow cytometry provides phenotype data and does not prove mechanism and this leaves open multiple mechanistic possibilities as discussed and explored through in vitro studies. While the mechanistic studies provided in this manuscript are not exhaustive, the cytotoxicity assay does demonstrate that PLC ϵ 1 expression in T cells does not contribute to cytotoxic function and the chemotaxis assay does demonstrate that in the absence of PLC ϵ 1, in both human and murine T cells, chemotaxis is significantly decreased. Overall, the data included in this manuscript shows that MC38 tumors are larger in mice that do not express PLC ϵ 1, the T cell ratio is altered in multiple anatomic compartments in tumor-bearing PLC ϵ 1 knockout mice, T cell activation is decreased in multiple anatomic compartments in tumor-bearing PLC ϵ 1 knockout mice, PLC ϵ 1 knockout T cells maintain cytotoxic function, and PLC ϵ 1 depleted T cells do not respond to chemotactic stimuli to the same extent as wild type T cells. From this data collectively as well as the known literature on PLC ϵ 1, we conclude that PLC ϵ 1 expression in T cells may contribute to an anti-tumor immune response.

It would be of interest to assess the combined impact of PLC ϵ 1 activation with checkpoint inhibition within a tumor model given that enhanced tumor infiltration is critical to T cell mediated tumor clearance. A recent study published in *Immunity* took the first steps in linking the chemokine network with anti-PD-1 treatment. Their work concludes that CXCR3 expression on CD8⁺ T cells is critical for proper localization within the tumor and anti-PD-1 efficacy [21]. With further work to uncover the mechanism underlying the role for PLC ϵ 1 in these chemokine pathways we put forth that local activation of PLC ϵ 1 within T cells may be a viable therapeutic strategy in the treatment of solid tumors.

Figure legends

Figure 1. PLC ϵ 1 limits MC38 tumor growth and contributes to T cell subset distribution. a) MC38 tumor volume calculated daily. n=14 PLC ϵ 1 KO mice from 3 independent experiments with n \geq 3 mice per experiment, n=22 WT mice from 4 independent

experiments with $n \geq 5$ mice per experiment; points represent mean \pm SEM. **b-e**) Cells from spleens of normal **(b)** and tumor-bearing **(c)** mice along with the right inguinal lymph nodes **(d)** and tumors **(e)** from tumor-bearing mice were isolated and stained for CD3, CD4, and CD8 then analyzed by flow cytometry. Events were gated for live CD3⁺ events then CD4⁺ or CD8⁺; populations shown are total CD3⁺, CD3⁺ CD4⁺ CD8⁻, CD3⁺ CD4⁻ CD8⁺. $n=4$ WT and PLC ϵ 1 KO mice from 2 independent experiments with 2 mice per experiment per group; bars represent mean \pm SEM. * $p \leq 0.05$, ** $p \leq 0.01$, *** $p \leq 0.001$, **** $p \leq 0.0001$, $p > 0.05$ not indicated.

Figure 2. Activation of tumor infiltrating T cells requires PLC ϵ 1. Cells from spleens, lymph nodes, and tumors from tumor-bearing mice were isolated and stained for CD3, CD4, CD8, CD44, PD-1, and CD62L then analyzed by flow cytometry. Events were gated for live CD3⁺ events then CD4⁺ CD8⁻ **(a, b)** or CD4⁻ CD8⁺ **(c, d)**. $n=4$ of WT and PLC ϵ 1 KO mice from 2 independent experiments with 2 mice per experiment per group. LN (Lymph nodes). Bars represent mean \pm SEM. * $p \leq 0.05$, ** $p \leq 0.01$, *** $p \leq 0.001$, **** $p \leq 0.0001$, $p > 0.05$ not indicated.

Figure 3. Infiltrating CD4⁺ T cells express different chemokine receptors in the absence of PLC ϵ 1. **a)** Splenocytes from WT and PLC ϵ 1 KO mice were stimulated with Staphylococcus Aureus Enterotoxin E (SEE) for 72 hours. Then CD8⁺ T cells were isolated and co-incubated with Raji cells and SEE for 4 hours after which LDH activity was quantified. Biological replicates were from $n=3$ WT mice, $n=5$ PLC ϵ 1 KO mice stimulated independently; points represent mean \pm SEM. **b)** Cells from spleens, right inguinal lymph nodes, and tumors were isolated and stained for CD3, CD4, CD8, CXCR4, CCR4, and CXCR3 then analyzed by flow cytometry. Events were gated for live CD3⁺ events then CD4⁺ CD8⁻. $n=3-4$ WT and PLC ϵ 1 KO mice from 2 independent experiments with 2 mice per experiment per group; points represent mean \pm SEM. * $p \leq 0.05$ based on comparison between WT and KO for individual chemokine receptors (indicated by dotted line), $p > 0.05$ not indicated. **c)** Primary murine CD3⁺ T cells transfected with siRNA non-targeting (siScramble) or PLC ϵ 1 (siPLC ϵ 1) were added to the apical chamber of transwell inserts with SDF-1 α containing media in the

basolateral chamber. After 3 hours cells in the basolateral chamber were quantified. n=3 independent experiments, each performed in duplicate. Bars indicate mean \pm SEM; *p \leq 0.05.

References

1. Khan H, Pillarisetty VG, Katz SC. The prognostic value of liver tumor T cell infiltrates. *J Surg Res* 2014; **191**:189-95.
2. Peske JD, Woods AB, Engelhard VH. Control of CD8 T-Cell Infiltration into Tumors by Vasculature and Microenvironment. *Adv Cancer Res* 2015; **128**:263-307.
3. Stanton SE, Disis ML. Clinical significance of tumor-infiltrating lymphocytes in breast cancer. *Journal for immunotherapy of cancer* 2016; **4**:59.
4. de Ruiter EJ, Ooft ML, Devriese LA, Willems SM. The prognostic role of tumor infiltrating T-lymphocytes in squamous cell carcinoma of the head and neck: A systematic review and meta-analysis. *Oncoimmunology* 2017; **6**:e1356148.
5. Sharma P, Allison JP. The future of immune checkpoint therapy. *Science* 2015; **348**:56-61.
6. Oelkrug C, Ramage JM. Enhancement of T cell recruitment and infiltration into tumours. *Clin Exp Immunol* 2014; **178**:1-8.
7. Atretkhany KN, Drutskaya MS, Nedospasov SA, Grivennikov SI, Kuprash DV. Chemokines, cytokines and exosomes help tumors to shape inflammatory microenvironment. *Pharmacol Ther* 2016; **168**:98-112.
8. Strazza M, Mor A. Consider the chemokines: a review of the interplay between chemokines and T cell subset function. *Discov Med* 2017; **24**:31-9.
9. Schall TJ, Proudfoot AE. Overcoming hurdles in developing successful drugs targeting chemokine receptors. *Nat Rev Immunol* 2011; **11**:355-63.
10. Gladue RP, Brown MF, Zwillich SH. CCR1 antagonists: what have we learned from clinical trials. *Curr Top Med Chem* 2010; **10**:1268-77.
11. Zhang J, Romero J, Chan A, Goss J, Stucka S, Cross J, Chamberlain B, Varoglu M, Chandonnet H, Ryan D, Lippa B. Biarylsulfonamide CCR9 inhibitors for inflammatory bowel disease. *Bioorg Med Chem Lett* 2015; **25**:3661-4.

12. Feagan BG, Sandborn WJ, D'Haens G, Lee SD, Allez M, Fedorak RN, Seidler U, Vermeire S, Lawrance IC, Maroney AC, Jurgensen CH, Heath A, Chang DJ. Randomised clinical trial: vercirnon, an oral CCR9 antagonist, vs. placebo as induction therapy in active Crohn's disease. *Aliment Pharmacol Ther* 2015; **42**:1170-81.
13. Strazza M, Azoulay-Alfaguter I, Peled M, Smrcka AV, Skolnik EY, Srivastava S, Mor A. PLCepsilon1 regulates SDF-1alpha-induced lymphocyte adhesion and migration to sites of inflammation. *Proc Natl Acad Sci U S A* 2017; **114**:2693-8.
14. Kalwa H, Storch U, Demleitner J, Fiedler S, Mayer T, Kannler M, Fahlbusch M, Barth H, Smrcka A, Hildebrandt F, Gudermann T, Dietrich A. Phospholipase C epsilon (PLCepsilon) induced TRPC6 activation: a common but redundant mechanism in primary podocytes. *J Cell Physiol* 2015; **230**:1389-99.
15. Sadowski CE, Lovric S, Ashraf S, Pabst WL, Gee HY, Kohl S, Engelmann S, Vega-Warner V, Fang H, Halbritter J, Somers MJ, Tan W, Shril S, Fessi I, Lifton RP, Bockenhauer D, El-Desoky S, Kari JA, Zenker M, Kemper MJ, Mueller D, Fathy HM, Soliman NA, Group SS, Hildebrandt F. A single-gene cause in 29.5% of cases of steroid-resistant nephrotic syndrome. *J Am Soc Nephrol* 2015; **26**:1279-89.
16. Tyutyunnykova A, Telegeev G, Dubrovskaya A. The controversial role of phospholipase C epsilon (PLCepsilon) in cancer development and progression. *J Cancer* 2017; **8**:716-29.
17. Wang H, Oestreich EA, Maekawa N, Bullard TA, Vikstrom KL, Dirksen RT, Kelley GG, Blaxall BC, Smrcka AV. Phospholipase C epsilon modulates beta-adrenergic receptor-dependent cardiac contraction and inhibits cardiac hypertrophy. *Circ Res* 2005; **97**:1305-13.
18. Cossarizza A, Chang HD, Radbruch A, Akdis M, Andra I, Annunziato F, Bacher P, Barnaba V, Battistini L, Bauer WM, Baumgart S, Becher B, Beisker W, Berek C, Blanco A, Borsellino G, Boulais PE, Brinkman RR, Buscher M, Busch DH, Bushnell TP, Cao X, Cavani A, Chattopadhyay PK, Cheng Q, Chow S, Clerici M, Cooke A, Cosma A, Cosmi L, Cumano A, Dang VD, Davies D, De Biasi S, Del Zotto G, Della Bella S, Dellabona P, Deniz G, Dessing M, Diefenbach A, Di Santo J, Dieli F, Dolf A, Donnerberg VS, Dorner T, Ehrhardt GRA, Endl E, Engel P, Engelhardt B, Esser C, Everts B, Dreher A, Falk CS,

Fehniger TA, Filby A, Fillatreau S, Follo M, Forster I, Foster J, Foulds GA, Frenette PS, Galbraith D, Garbi N, Garcia-Godoy MD, Geginat J, Ghoreschi K, Gibellini L, Goettlinger C, Goodyear CS, Gori A, Grogan J, Gross M, Grutzkau A, Grummitt D, Hahn J, Hammer Q, Hauser AE, Haviland DL, Hedley D, Herrera G, Herrmann M, Hiepe F, Holland T, Hombrink P, Houston JP, Hoyer BF, Huang B, Hunter CA, Iannone A, Jack HM, Javega B, Jonjic S, Juelke K, Jung S, Kaiser T, Kalina T, Keller B, Khan S, Kienhofer D, Kroneis T, Kunkel D, Kurts C, Kvistborg P, Lannigan J, Lantz O, Larbi A, LeibundGut-Landmann S, Leipold MD, Levings MK, Litwin V, Liu Y, Lohoff M, Lombardi G, Lopez L, Lovett-Racke A, Lubberts E, Ludewig B, Lugli E, Maecker HT, Martrus G, Matarese G, Maueroder C, McGrath M, McInnes I, Mei HE, Melchers F, Melzer S, Mielenz D, Mills K, Mirrer D, Mjosberg J, Moore J, Moran B, Moretta A, Moretta L, Mosmann TR, Muller S, Muller W, Munz C, Multhoff G, Munoz LE, Murphy KM, Nakayama T, Nasi M, Neudorfl C, Nolan J, Nourshargh S, O'Connor JE, Ouyang W, Oxenius A, Palankar R, Panse I, Peterson P, Peth C, Petriz J, Philips D, Pickl W, Piconese S, Pinti M, Pockley AG, Podolska MJ, Pucillo C, Quataert SA, Radstake T, Rajwa B, Rebhahn JA, Recktenwald D, Remmerswaal EBM, Rezvani K, Rico LG, Robinson JP, Romagnani C, Rubartelli A, Ruckert B, Ruland J, Sakaguchi S, Sala-de-Oyanguren F, Samstag Y, Sanderson S, Sawitzki B, Scheffold A, Schiemann M, Schildberg F, Schimisky E, Schmid SA, Schmitt S, Schober K, Schuler T, Schulz AR, Schumacher T, Scotta C, Shankey TV, Shemer A, Simon AK, Spidlen J, Stall AM, Stark R, Stehle C, Stein M, Steinmetz T, Stockinger H, Takahama Y, Tarnok A, Tian Z, Toldi G, Tornack J, Traggiai E, Trotter J, Ulrich H, van der Braber M, van Lier RAW, Veldhoen M, Vento-Asturias S, Vieira P, Voehringer D, Volk HD, von Volkman K, Waisman A, Walker R, Ward MD, Warnatz K, Warth S, Watson JV, Watzl C, Wegener L, Wiedemann A, Wienands J, Willimsky G, Wing J, Wurst P, Yu L, Yue A, Zhang Q, Zhao Y, Ziegler S, Zimmermann J. Guidelines for the use of flow cytometry and cell sorting in immunological studies. *Eur J Immunol* 2017; **47**:1584-797.

19. Sierra-Filardi E, Nieto C, Dominguez-Soto A, Barroso R, Sanchez-Mateos P, Puig-Kroger A, Lopez-Bravo M, Joven J, Ardavin C, Rodriguez-Fernandez JL, Sanchez-Torres C, Mellado M, Corbi AL. CCL2 shapes macrophage polarization by GM-CSF

- and M-CSF: identification of CCL2/CCR2-dependent gene expression profile. *J Immunol* 2014; **192**:3858-67.
20. Weigel E SC, Liu PG, Robison R, O'Neill K. Macrophage Polarization and Its Role in Cancer. *J Clin Cell Immunol* 2015; **6**.
 21. Chow MT, Ozga AJ, Servis RL, Frederick DT, Lo JA, Fisher DE, Freeman GJ, Boland GM, Luster AD. Intratumoral Activity of the CXCR3 Chemokine System Is Required for the Efficacy of Anti-PD-1 Therapy. *Immunity* 2019.

Disclosure of potential conflicts of interest

None.

Acknowledgments

This research was supported by grants to A.M. (NIH R01 AI125640, NIH CA231277, and the Cancer Research Institute). Research reported in this publication was performed in the CCTI Flow Cytometry Core, supported in part by the Office of the Director, National Institutes of Health under awards S10RR027050 and S10OD020056.

Author's contributions

Conception and design: M.S. and A.M. *Development of methodology:* M.S., K.A., A.S., S.L., and A.M. *Acquisition of data:* M.S., A.S., and A.M. *Analysis and interpretation of data:* M.S. and A.M. *Writing, review, and/or revision of the manuscript:* M.S. and A.M. *Administrative, technical, or material support:* M.S. and K.A. *Study supervision:* M.S. and A.M.

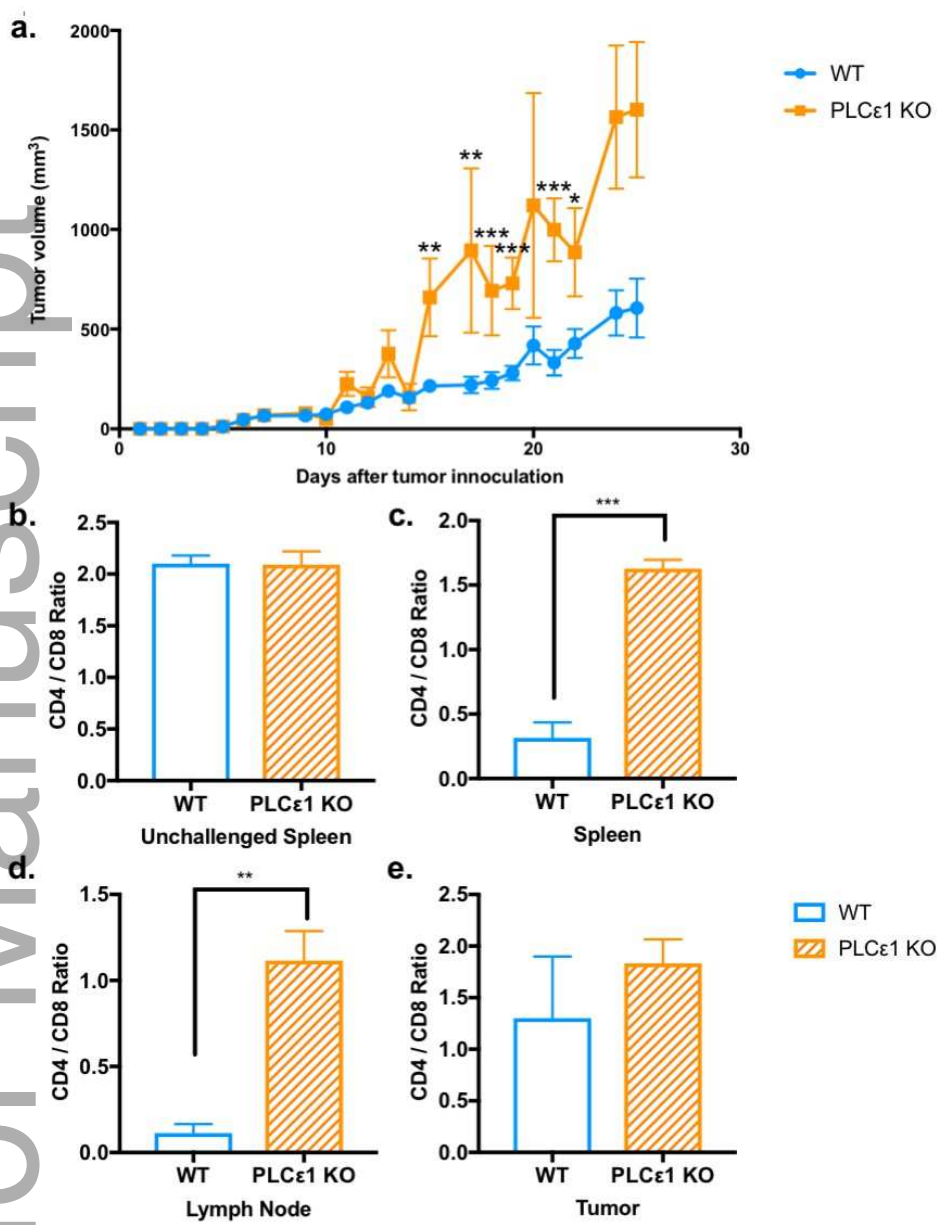


Figure 1

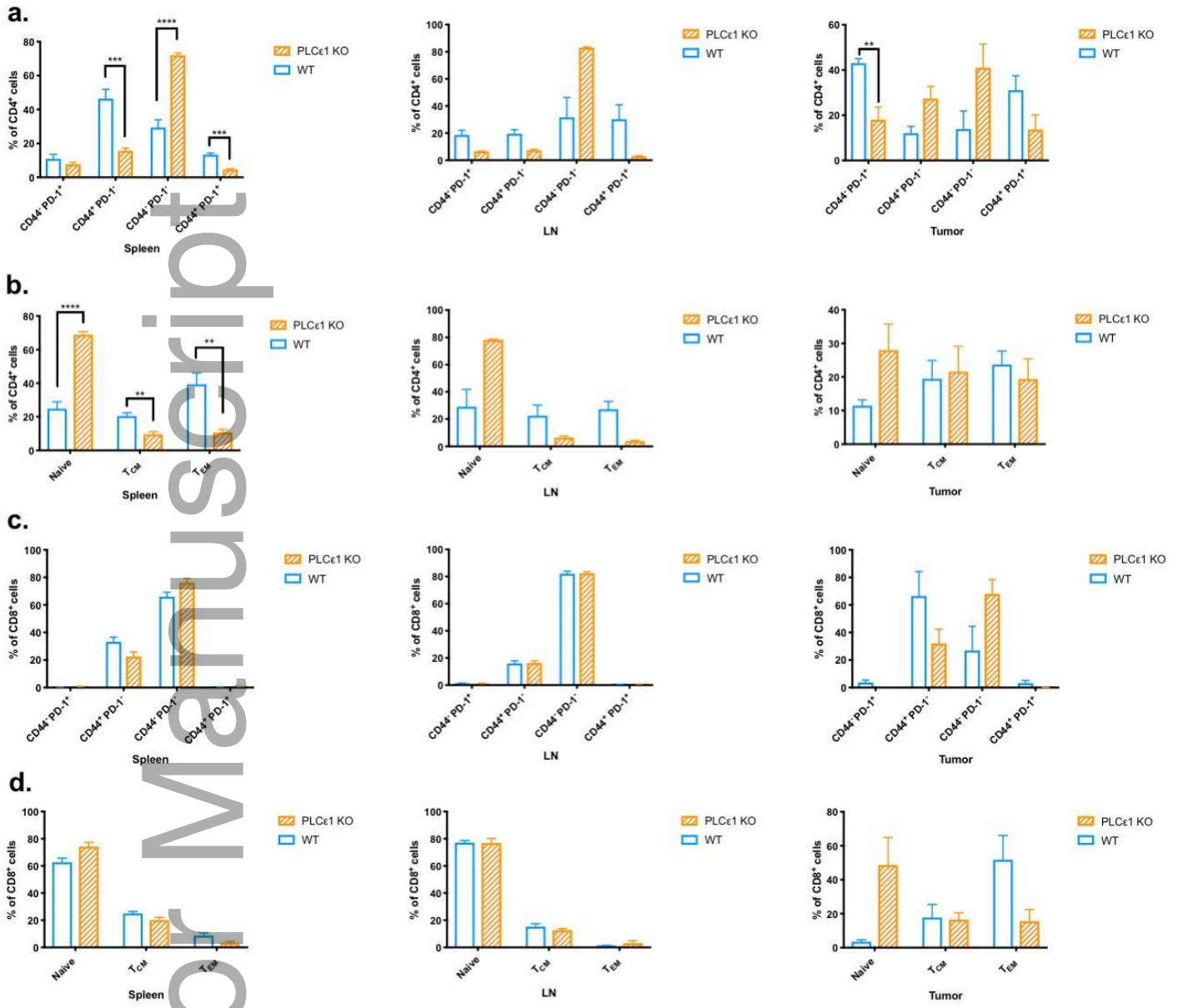


Figure 2

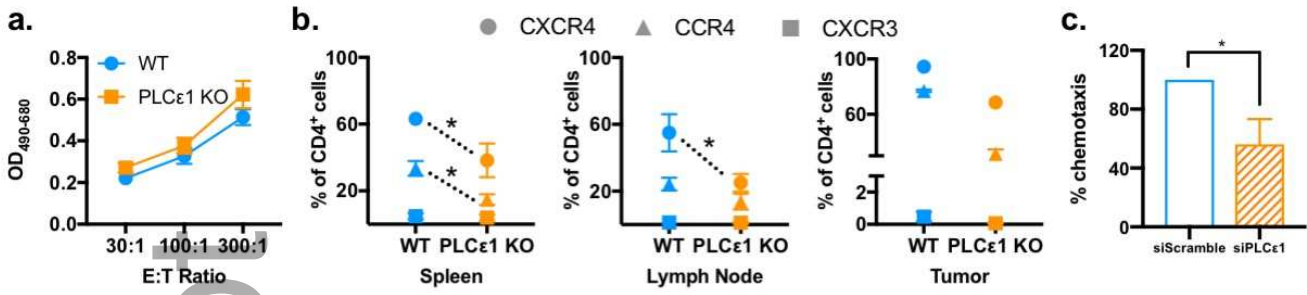


Figure 3